Extremophiles
https://doi.org/10.1007/s00792-018-1030-y

ORIGINAL PAPER

Prokaryotic and eukaryotic community structure affected by the presence of an acid mine drainage from an abandoned gold mine

José O. Bonilla[1,2] · Daniel G. Kurth[3] · Fabricio D. Cid[2,4] · José H. Ulacco[5] · Raúl A. Gil[1,2] · Liliana B. Villegas[1,2]

Received: 2 February 2018 / Accepted: 20 April 2018

Abstract

The acid mine drainage that originates in the abandoned gold mine in San Luis, Argentina, is released into La Carolina stream. The aim of this study was to determine the influence of this mine drainage on the physicochemical parameters of the area studied and on both prokaryotic and eukaryotic community structure. In addition, specific relationships between microbial taxonomic groups and physicochemical parameters were established. The drainage that flows into La Carolina stream acidifies the stream and increases its sulfate, Zn, Cd and Te concentrations. Microbial analysis showed that prokaryotic community structure is mainly affected by pH values. *Actinobacteria* and *Gammaproteobacteria* were abundant in samples characterized by low pH values, while *Nitrospirae, Chloroflexi, Deltaproteobacteria, Thaumarchaeota* and *Euryarchaeota* were associated with high concentrations of heavy metals. Otherwise, *Alphaproteobacteria* was present in samples taken in sunlit areas. Regarding eukaryotic community structure, the sunlight had the greatest impact. Inside the mine, in the absence of light, fungi and protists members were the most abundant microorganisms, while those samples taken in the presence of light displayed algae (green algae and diatoms) as the most abundant ones. After receiving the mine drainage, the stream showed a decrease in the diatom abundance and green algae predominated.

Keywords Acid mine drainage · Mining environmental liabilities · Eukaryotic community structure · Prokaryotic community structure · Metagenomics

Introduction

Acid mine drainage (AMD) refers to the acidic water produced in both active and abandoned mines where acid-forming minerals are exposed at the earth surface and this is the most frequently documented type of water pollution associated with mining activities (Johnson and Hallberg 2003; Méndez-García et al. 2015). This acidic water is produced from oxidative dissolution of sulfide ores exposed to oxygen, water and endogenous microorganisms. The most common sulfides present in mining areas are pyrite (FeS_2) and arsenopyrite (FeAsS) (Kirschbaum et al. 2012). At low pH, ferric ion is the predominant oxidant and autochthonous acidophilic microorganisms can mediate its production and conserve energy from its redox transformations (Bond et al. 2000), making this relation an environmental problem.

AMDs are generally characterized by the presence of heavy metals. Low pH water enhances the mobility of heavy metals and converts them into potential pollutants to soils, sediments, terrestrial plants and it is capable of causing

José O. Bonilla and Daniel G. Kurth have contributed equally to this work.

Communicated by L. Huang.

Electronic supplementary material The online version of this article (https://doi.org/10.1007/s00792-018-1030-y) contains supplementary material, which is available to authorized users.

✉ Liliana B. Villegas
lbvilleg@gmail.com; labmicrobiolamb.inquisal@gmail.com

1 Instituto de Química San Luis (INQUISAL), CONICET, San Luis, Argentina

2 Facultad de Química, Bioquímica y Farmacia, Universidad Nacional de San Luis, San Luis, Argentina

3 Planta Piloto de Procesos Industriales y Microbiológicos (PROIMI), CONICET, Tucumán, Argentina

4 Instituto Multidisciplinario de Investigaciones Biológicas de San Luis (IMIBIOSL), CONICET, San Luis, Argentina

5 Departamento de Geología, Universidad Nacional de San Luis, San Luis, Argentina

Published online: 28 April 2018

adverse effects to life in general (Fadiran et al. 2014). Although heavy metals can be found in these environments at very low concentrations, it must be borne in mind that long exposure times can cause their accumulation in water bodies or sediments, reaching pollution levels (Jennings et al. 2008). The study of heavy metal concentrations in sediments is crucial given the fact that sediments are basic ecological components of aquatic habitats and act as reservoirs for pollutants. They play a significant role in maintaining the trophic status of water bodies (Singh et al. 1997).

It is also known that AMD affected environments are low-complexity natural systems in terms of biodiversity, as reviewed by Méndez-García et al. 2015. Temperature, total organic carbon, pH, dissolved oxygen and other solutes such as heavy metals significantly influence microbial life in water bodies or sediments (Edwards et al. 1999). In these environments, extreme conditions contribute to the reduction of diversity and abundance of different species and the pH is one of the major forces that produces this variation (Kuang et al. 2013). The balance of the members of a microbial community is affected because the presence of pollutants results in a decrease in sensitive populations in AMD affected environments (Hernandez and Pastor 2008).

Most studies have focused on microbial community structure analysis of AMD affected sites, mostly including organisms belonging to Bacteria and Archaea, and only a few dedicated to the study of Eukarya (predominantly fungi and algae) (Méndez-García et al. 2015). However, little is known about the specific relations between physicochemical parameters and microbial taxonomic groups. Understanding the distribution and metabolisms of species present in extreme environments such as AMD affected environments is essential to develop bioremediation processes of contaminated sites.

"Mining Environmental Liabilities" (MEL) is a term coined in Latin America which includes all installations, effluents, emissions, remains or waste deposits produced by mining operations, which now are abandoned or inactive, and constitute a permanent and potential risk for the population health and for the ecosystem and property (Oblasser and Chaparro Ávila 2008). Similar definitions are used in other countries such as Canada and the USA (EPA United States Environmental Protection Agency 2017), taking into account different criteria. In La Carolina (San Luis, Argentina), there is an abandoned gold mine called "La Esperanza". This is a vetiform gold deposit, whose mineralization consists of disseminated pyrite, native gold, and galena and sphalerite in a smaller proportion. In this deposit, extractions were carried out intermittently until 1894. As a result of its exploitation, galleries and facilities have been abandoned with no appropriate closure process, constituting MEL. The drainage released from this mine possesses AMD characteristics (Tripole and Corigliano 2005, Tripole et al. 2006), and water flows into the La Carolina stream, which is used for recreational and touristic activities.

This study has a twofold objective: on the one hand, to determine the influence of the AMD released into La Carolina stream on the determined physicochemical parameters of the stream sediments; on the other, to establish specific relations between microbial taxonomic groups and physicochemical characteristics of the affected area to describe the environmental conditions that favor the presence of some microbial groups over others.

Materials and methods

Sampling

A total of 28 sediment samples were taken from the abandoned gold mine in La Carolina, San Luis, Argentina (−32.804904, −66.085954), as shown in Fig. 1. Sediments were obtained from surface sediment fraction (0–10 cm deep), as follows:

- From inside the mine, 12 samples were taken: five samples (separated by 60 m one from the other) were taken from the main gallery (M1–M5). Other four samples in the lateral galleries (M6–M9) and three samples in the south gallery (M10–M12), each sample separated by 20 m one from the other.
- Sixteen samples were taken from La Carolina stream bed, which receives the AMD, separated by 100 m one from another: seven samples were taken up-stream from the mine (R1–R7), five intermediate stream samples were taken between main gallery and south gallery drainages (R8–R12), and finally, four samples were taken downstream from the mine (R13–R16). Samples R1–R7 were taken as reference to study the zone not affected by the mining activities.

All samples were collected in amber vials for their physicochemical analysis and in sterile tubes for their microbiological studies. Distances between stream sampling points were determined by GPS reference. Inside the mine, distances were determined using a 10 m measuring tape.

Zone description

The clasts of the stream sediments are made up of schists and volcanites, with a predominance of the last ones. The fragments are subangular or rounded. The predominant fractions in the sediments are the gravels with a percentage of 80–85%, presenting an average size of 6 cm. These are composed of volcanic and metamorphic rocks in a greater proportion, followed by fragments of pegmatites. Volcanites

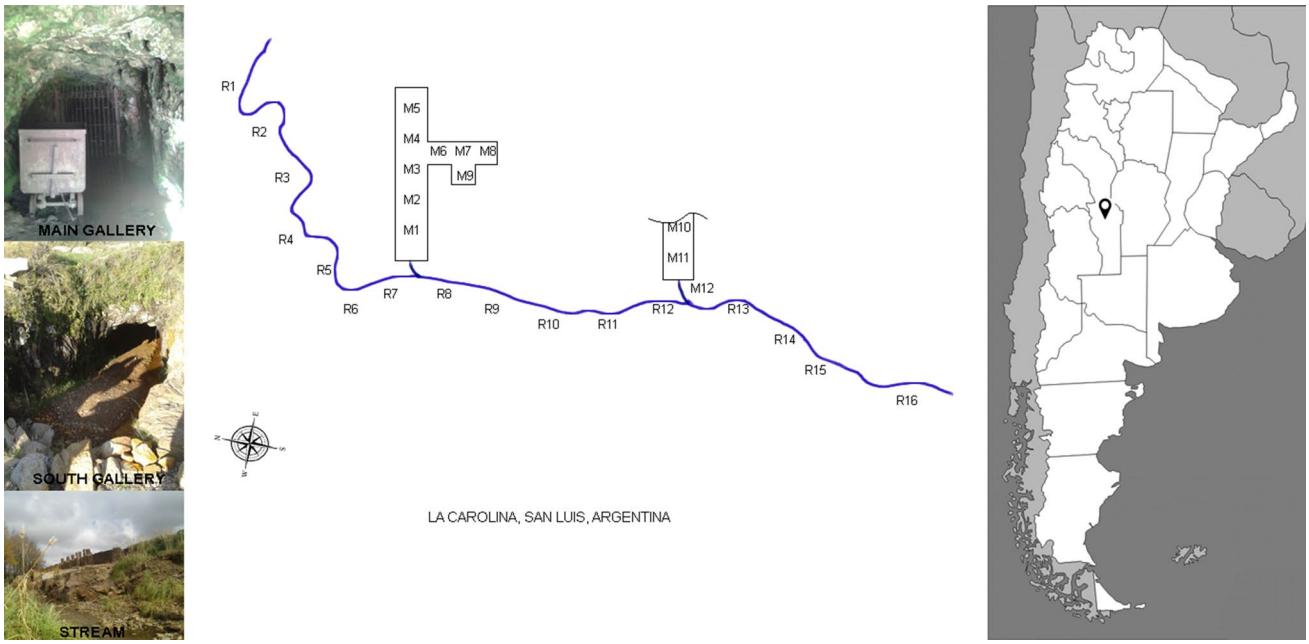

Fig. 1 Sampling points around the abandoned gold mine. M refers to the samples taken from the mine galleries and R refers to the samples taken from the stream. Distribution of samples: Main gallery (M1–5), lateral galleries (M6–9), south gallery (M10–12), up-stream samples (R1–7), intermediate stream samples (R8–R12), and down-stream samples (R13–16). The stream flows from the left to the right in the figure

are found in proportions between 50 and 70%, increasing their proportion down-stream from the mine. In the vulcanite clasts, it is common to see imprints of leached sulfide ores.

The fine fractions (sand, silt and clay) are present in proportions of 10–35%. The sand composition corresponds mainly to volcanic rocks, fragments of quartz and feldspar, and only few metamorphites. Silt and clay are present in very low proportions.

The fine sediments are agglutinated with gels and/or concretions of reddish brown iron oxides in the samples taken after receiving the drainage from the mine. They form thicknesses of up to 15 cm in some sectors. The stream samples present total organic carbon (TOC) between 2.40 and 17.5%.

The sediments taken from the mine have a predominance of medium to fine sand (54%), coarse sand (10%), and the rest consists of silts, clays and ocher concretions-aggregates. The thick clasts are composed of schists and volcanites, with brown-yellow patinas. In the medium to fine sand fraction, quartz and mica predominate. In mine samples, the TOC values range from 0.4 to 0.7%.

The stream, up-stream from the mine, has a flow rate of 0.053 $m^3\ s^{-1}$. On the other hand, drainages from the main and south galleries are both 0.0024 $m^3\ s^{-1}$. Flow rates were determined in spring.

Dissolved oxygen values were 7.58 mg L^{-1} (up-stream samples), 7.28 mg L^{-1} (intermediate stream samples), 8.36 mg L^{-1}(down-stream samples), 4.82 mg L^{-1}(main gallery samples), 9.84 mg L^{-1} (lateral galleries samples) and 7.08 mg L^{-1} (south gallery samples).

Physicochemical parameters determination

All samples were dried in an oven at 65 °C during 24 h. Through batch leaching test, the determination of soluble heavy metal concentrations was performed (Tiwari et al. 2015). Solutions of NaOH and H_2SO_4 were used to simulate environmental conditions of pH when sampling was carried out. 1 g dry mass of each sample was placed in solution in a liquid–solid ratio 10:1 (L/S = 10) (Ruggieri et al. 2012). Each sample was incubated for 4 h at 18 °C and 180 rpm. Finally, solutions were filtered in vacuum and the determination of 15 soluble heavy metal concentrations (Mo, Cr, Mn, Fe, Co, Ni, Cu, Zn, As, Ag, Te, Au, Hg, Pb and Cd) was performed by inductively coupled plasma mass spectrometry (ICP-Mass ELAN DRC-e). QA/QC procedures were carried out as it is recommended by Sciex-Perkin Elmer Eland DRC-e User manual.

Sulfate concentrations were determined from 100 g of dry soil. Saturated paste of sediment was filtered by means of Whatman filter paper. Sulfate concentrations were determined in the filtrated solutions by the turbidimetric method Sulfaver®4 for 10 mL using HACH DR 2800. The pH values were determined using the Waterproof tester HI 98121-HANNA.

Results were analyzed by multivariate statistical technique (PCA–Principal Components Analysis) to determine the influence of the released AMD on physicochemical parameters of La Carolina stream.

Microbial community structure study

To perform the analysis of microbial community structure, 12 sediment samples were selected for DNA extraction. Samples stream sediments R1, R4, R11, R13 and R16, and mine sediments M3, M5, M6, M8, M9, M10 and M12 were selected to cover all sites of the study area.

The total DNA was isolated using the Power Soil DNA Isolation Kit, MOBIO (12888-50). Its purity was checked with A260:A280 ratio (Epoch, Biotek). DNA concentration was also calculated from optical density data. The integrity of the samples was evaluated in 1% agarose gel.

The 16S rRNA gene and the 18S rRNA gene with barcode on the forward primers (515F/806R and 7F/570R, respectively) were used in a 30 cycle PCR to amplify the fragments using the Hot Start Taq Plus Master Mix Kit (Qiagen, USA) under the following conditions: 94 °C for 3 min, followed by 28 cycles of 94 °C for 30 s, 53 °C for 40 s and 72 °C for 1 min, after which a final elongation step at 72 °C for 5 min was performed. After amplification, PCR products were checked in 2% agarose gel to determine the success of the amplification and the relative intensity of bands. Pooled samples were purified using calibrated Ampure XP beads. Then, the pooled and purified PCR product was used to prepare the DNA library by following Illumina TruSeq DNA library preparation protocol. Amplification, DNA library preparation and sequencing were performed at MR DNA (www.mrdnalab.com, Shallowater, TX, USA) on a MiSeq (Illumina) following the manufacturer's guidelines. Sequence data were processed using MR DNA analysis pipeline (MR DNA, Shallowater, TX, USA). In summary, sequences were joined, depleted of barcodes, then sequences < 150 bp and sequences with ambiguous base calls were removed. Further analyses were performed with the NGS analysis pipeline of the SILVA rRNA gene database project (SILVAngs 1.3) (https://www.arb-silva.de/ngs) (Quast et al. 2013) and MG-RAST 3.6 (http://metagenomics.anl.gov) (Meyer et al. 2008), with their default pipeline parameters. On MG-RAST server, using the web application to create heatmaps, Bray–Curtis distances were evaluated between every possible pair of samples classified at class level, and ward-based clustering produced dendrogram trees.

Sequence read accession numbers

All sequence data were deposited into NCBI Sequence Read Archive under BioProject number PRJNA306428: Sediment of acid mine drainage targeted loci environmental.

SRA Run accession numbers SRR3032156 (R1), SRR3032056 (R4), SRR3032148 (R11), SRR3032152 (R13), SRR3032153 (R16), SRR3032155 (M3), SRR3032053 (M5), SRR3032157 (M6), SRR3032147 (M8), SRR3032058 (M9), SRR3032154 (M10) and SRR3032150 (M12) correspond to 16S rRNA gene metagenomics sequence data.

SRA Run accession numbers SRR3032417 (R1), SRR3032408 (R4), SRR3032411 (R11), SRR3032413 (R13), SRR3032414 (R16), SRR3032416 (M3), SRR3032407 (M5), SRR3032418 (M6), SRR3032410 (M8), SRR3032409 (M9), SRR3032415 (M10) and SRR3032412 (M12) correspond to 18S rRNA gene metagenomics sequence data.

Canonical correspondence analysis

The correlation of environmental variables with microbial taxa and samples was analyzed by canonical correspondence (CCA), using the CANOCO 4.5 software package (Microcomputer Power, Ithaca, NY, USA). Significance of the canonical axes was determined by Monte Carlo test with 499 permutations. Triplot graphs were generated for visualization of the results. OTUs were merged according to their taxonomic classification, and only taxa with abundances above 0.2 and 1% were considered for prokaryotic and eukaryotic data, respectively. OTUs assigned to mitochondria and chloroplasts were not considered in the prokaryotic analysis. This analysis was also performed with phyla level abundances for prokaryotic sequences.

Results

Physicochemical parameters analysis

Physicochemical parameter values selected for PCA analysis are summarized in Table 1. As shown in Fig. 2, the PCA of soluble heavy metals and physicochemical parameters such as sulfate ion content and pH values displayed samples in three major groups. The first group that includes the lateral galleries samples (M6, M7, M8 and M9) was characterized by higher concentrations of Cu, Co, Ni, Pb, Fe, Mn, Hg, Cr and lower pH values than the other groups. The second group, including south gallery (M10, M11 y M12) and down-stream samples (R13–R16) contained high concentrations of sulfate ions, Zn, Cd and Te. Finally, the third group of samples from the main gallery (M1–M5) and stream samples (R1–R12) had pH values between 6.42 and 8.05 and slightly high concentrations of Au, Mo and Ag.

From these results, it can be clearly observed that the drainage of the southern gallery released into La Carolina stream influences on its physicochemical characteristics,

Table 1 Physicochemical parameter values grouped by sampling zones (mean, standard deviation, and minimum and maximum values)

	Main gallery (M1–M5)	Lateral galleries (M6–M9)	South gallery (M10–M12)	Up-stream (R1–R7)	Intermediate stream (R8–R12)	Down-stream (R13–R16)
Mo	0.001 ± 0.000 (0.000–0.002)	0.001 ± 0.001 (0.000–0.002)	0.000 ± 0.000 (0.000–0.000)	0.008 ± 0.003 (0.004–0.013)	0.004 ± 0.002 (0.002–0.006)	0.000 ± 0.000 (0.000–0.000)
Cr	0.023 ± 0.021 (0.007–0.056)	0.529 ± 0.953 (0.014–1.957)	0.025 ± 0.007 (0.019–0.033)	0.071 ± 0.025 (0.051–0.112)	0.042 ± 0.017 (0.024–0.067)	0.056 ± 0.016 (0.041–0.076)
Mn	21.535 ± 36.487 (2.220–86.681)	65.447 ± 22.592 (47.086–96.607)	29.153 ± 29.270 (11.923–62.949)	2.650 ± 1.108 (1.175–4.080)	25.390 ± 9.748 (12.365–36.683)	33.916 ± 14.188 (21.520–47.956)
Fe	1.365 ± 0.945 (0.315–2.512)	118.551 ± 133.684 (18.383–315.608)	105.606 ± 32.118 (74.388–138.553)	0.675 ± 0.231 (0.353–0.938)	0.946 ± 0.403 (0.543–1.550)	2.466 ± 0.452 (1.911–2.995)
Co	0.015 ± 0.026 (0.003–0.061)	0.271 ± 0.266 (0.051–0.624)	0.313 ± 0.0334 (0.108–0.698)	0.006 ± 0.003 (0.003–0.010)	0.032 ± 0.020 (0.018–0.066)	0.154 ± 0.075 (0.077–0.240)
Ni	0.074 ± 0.090 (0.022–0.234)	0.501 ± 0.504 (0.102–1.178)	0.362 ± 0.236 (0.214–0.634)	0.044 ± 0.012 (0.029–0.058)	0.073 ± 0.014 (0.058–0.094)	0.253 ± 0.079 (0.181–0.354)
Cu	0.067 ± 0.009 (0.051–0.073)	1.482 ± 1.107 (0.646–3.008)	1.045 ± 0.175 (0.843–1.162)	0.156 ± 0.036 (0.120–0.230)	0.132 ± 0.042 (0.097–0.199)	1.531 ± 0.515 (1.043–2.013)
Zn	1.199 ± 1.083 (0.460–3.009)	4.868 ± 3.364 (1.975–8.718)	9.382 ± 2.457 (6.802–11.693)	0.502 ± 0.150 (0.343–0.769)	0.728 ± 0.207 (0.513–0.991)	11.800 ± 3.756 (8.172–17.059)
As	0.034 ± 0.019 (0.018–0.063)	0.037 ± 0.032 (0.008–0.071)	0.005 ± 0.000 (0.005–0.006)	0.027 ± 0.012 (0.015–0.041)	0.032 ± 0.007 (0.025–0.043)	0.005 ± 0.001 (0.004–0.007)
Ag	0.001 ± 0.001 (0.000–0.002)	0.000 ± 0.000 (0.000–0.001)	0.001 ± 0.000 (0.000–0.001)	0.008 ± 0.003 (0.005–0.012)	0.009 ± 0.001 (0.008–0.012)	0.002 ± 0.000 (0.002–0.003)
Te	0.098 ± 0.063 (0.019–0.171)	0.415 ± 0.348 (0.181–0.924)	0.884 ± 0.253 (0.636–1.141)	0.072 ± 0.051 (0.000–0.129)	0.147 ± 0.023 (0.110–0.172)	0.639 ± 0.127 (0.551–0.827)
Au	0.000 ± 0.000 (0.000–0.000)	0.002 ± 0.003 (0.000–0.005)	0.000 ± 0.000 (0.000–0.000)	0.007 ± 0.005 (0.002–0.014)	0.001 ± 0.000 (0.000–0.002)	0.000 ± 0.000 (0.000–0.001)
Hg	0.001 ± 0.001 (0.000–0.002)	0.027 ± 0.013 (0.013–0.045)	0.005 ± 0.001 (0.005–0.006)	0.003 ± 0.002 (0.001–0.005)	0.002 ± 0.001 (0.001–0.003)	0.002 ± 0.000 (0.002–0.002)
Pb	0.000 ± 0.000 (0.000–0.000)	0.049 ± 0.043 (0.022–0.114)	0.041 ± 0.013 (0.033–0.056)	0.003 ± 0.002 (0.001–0.007)	0.001 ± 0.001 (0.000–0.002)	0.011 ± 0.005 (0.004–0.014)
Cd	0.002 ± 0.002 (0.001–0.005)	0.039 ± 0.023 (0.015–0.069)	0.059 ± 0.009 (0.051–0.069)	0.003 ± 0.003 (0.002–0.009)	0.003 ± 0.002 (0.002–0.006)	0.105 ± 0.034 (0.074–0.152)
Sulfate	17.562 ± 14.258 (9.761–42.945)	31.157 ± 14.778 (17.029–48.058)	218.281 ± 91.765 (128.500–311.909)	5.262 ± 2.390 (2.281–8.932)	7.132 ± 3.181 (3.842–10.770)	15.920 ± 5.469 (11.680–23.388)
pH	7.122 ± 0.091 (7.050–7.240)	3.603 ± 0.910 (2.910–4.940)	2.940 ± 0.026 (2.910–2.960)	7.957 ± 0.054 (7.870–8.050)	7.090 ± 0.417 (6.420–7.450)	5.013 ± 0.519 (4.650–5.780)

Values are presented as $\mu g\ g^{-1}$

mainly acidifying the stream and increasing its sulfate, Zn, Cd and Te concentrations. Heavy metals such as Pb, Cu, Fe, Cr and Hg are found inside the mine, especially in galleries where the regular tourism has no access (lateral and south galleries).

Microbial community structure study

Community structure was assessed by amplicon sequencing of 16S rRNA gene for prokaryotic community structure and 18S rRNA gene for eukaryotic community structure. Sequencing results are summarized in Online Resource 1. A Total of 848,997 and 470,679 sequences were obtained for 16S and 18S rRNA genes sequencing, respectively. Sequences were analyzed by the Silva NGS pipeline, which generated OTUs at 98% identity. The difference in sequencing depth was reflected in coverage: Good's coverage was better for 16S rRNA gene analysis. Moreover, rarefaction curves (Online Resource 2) for eukaryotic sequences showed a rather steep slope, suggesting that more sampling effort is required to catch the whole diversity. The steepness was less pronounced among prokaryotic sequences, and even a group of mine samples (M6, M8, M9, M10, M12) showed moderate slopes. This group also presented the highest values for Good's coverage.

Alpha diversity metrics were calculated using QIIME 1.9 scripts and the results are shown in Online Resource 3. OTU tables from the Silva NGS pipeline were rarefied and analyzed at the same sequencing depth for all samples. A pattern can be seen for prokaryotic samples. The highest richness (chao1, observed_species) and diversity (equitability, Shannon) indices were found in stream samples (R4, R11,

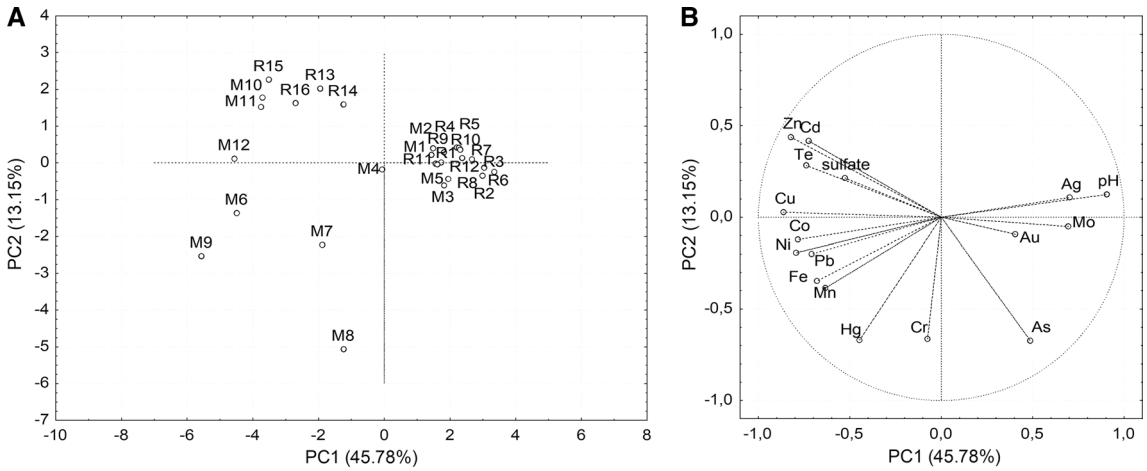

Fig. 2 Principal component analysis (PCA) defined by the first two axes (58.93%). Distribution of the sites (**a**) and of physicochemical variables (**b**)

R13). The lowest values for those indices were found in mine samples (M6, M8, M9, M10, M12). In addition, dominance was the highest on M10 and M12 samples, suggesting that fewer species are better represented in these samples. The pattern is less clear for eukaryotic samples, as the values showed less difference, but R11 and R16 showed the highest richness and diversity values, while M12 and R13 showed the maximum dominance.

Taxonomic assignment by the Silva NGS server is shown in Figs. 3 and 4. *Proteobacteria* were dominant in all samples, while other phyla such as *Acidobacteria*, *Nitrospirae* and *Cyanobacteria* were abundant in selected samples. Regarding eukaryotic data, R1, R4 and R11 samples were dominated by *SAR (Stramenopiles, Alveolata, Rhizaria),* mainly *Diatomea* (44–48%), while the samples from the most internal locations of the mine (M5, M6, M8, M10) had a high proportion of *Opisthokonta* (mostly *Fungi*, with 49% *Nematoda* only in M5). Likewise, *Archaeplastida* dominated the M12 sample. Unassigned reads were particularly abundant in the R13, M9 and M10 samples, suggesting that a rare eukaryotic community structure might be present in these locations. This is due to the stringent restrictions on the Silva NGS pipeline, which only classified reads with identity higher than 93% to database sequences. The unclassified reads have identities below 85%, with the most similar sequences affiliated to *Opisthokonta* in samples R13 and M9, and to *RT5iin25* group in sample M10. Even at this lower identity threshold, around 10% reads remained unclassified (data not shown).

Samples were grouped according to their similarities in microbial community structure using the MG-RAST server. Regarding prokaryotic community structure, MG-RAST server classified samples into four major groups (Fig. 3): R1, R4, R11, R13 and R16; M3 and M5; M6, M8, M9 and M10; and finally M12, collected in the south gallery of the mine. On the other hand, the study of microbial community structure with 18S rRNA gene sequence arrayed samples in two big groups according to their similarity in eukaryotic community structure, showing also significant differences between them (Fig. 4). One group of samples were M3, M5, M6, M8, M9 and M10, and the other group of samples were M12, R1, R4, R11, R13 and R16.

Considering that the distribution and grouping of samples were very different regarding microbial community structure with prokaryotic and eukaryotic analysis, a canonical correspondence analysis to relate physicochemical parameters with taxonomic groups was performed to know which physicochemical parameters were responsible for these differences in sample community structure.

Canonical correspondence analysis (CCA)

The Fig. 5 shows the CCA performed with the data obtained in the metagenomics analysis of 16S rRNA gene sequences at phylum and class levels for a better visualization. According to these results, samples were separated in two groups along the X axis: M6, M8, M9, M10 and M12 on the right side, and the stream samples tightly clustered on the left, with M3 and M5 samples close to them. Similar results were obtained at the lowest levels.

Actinobacteria (0.8–9.4% relative abundance per sample) and *Gammaproteobacteria* (3.7–41.6%) were present mainly in samples M10 and M12 (south gallery), characterized by low pH values and high concentrations of sulfate ions. *Cyanobacteria* (0.2–14.2%), *Bacteroidetes* (0.2–7.8%), *Betaproteobacteria* (0.7–28.6%) and *Verrucomicrobia* (0.1–8.8%) were present principally in samples obtained in the stream (R1, R4, R11, R13 and R16) and in the main

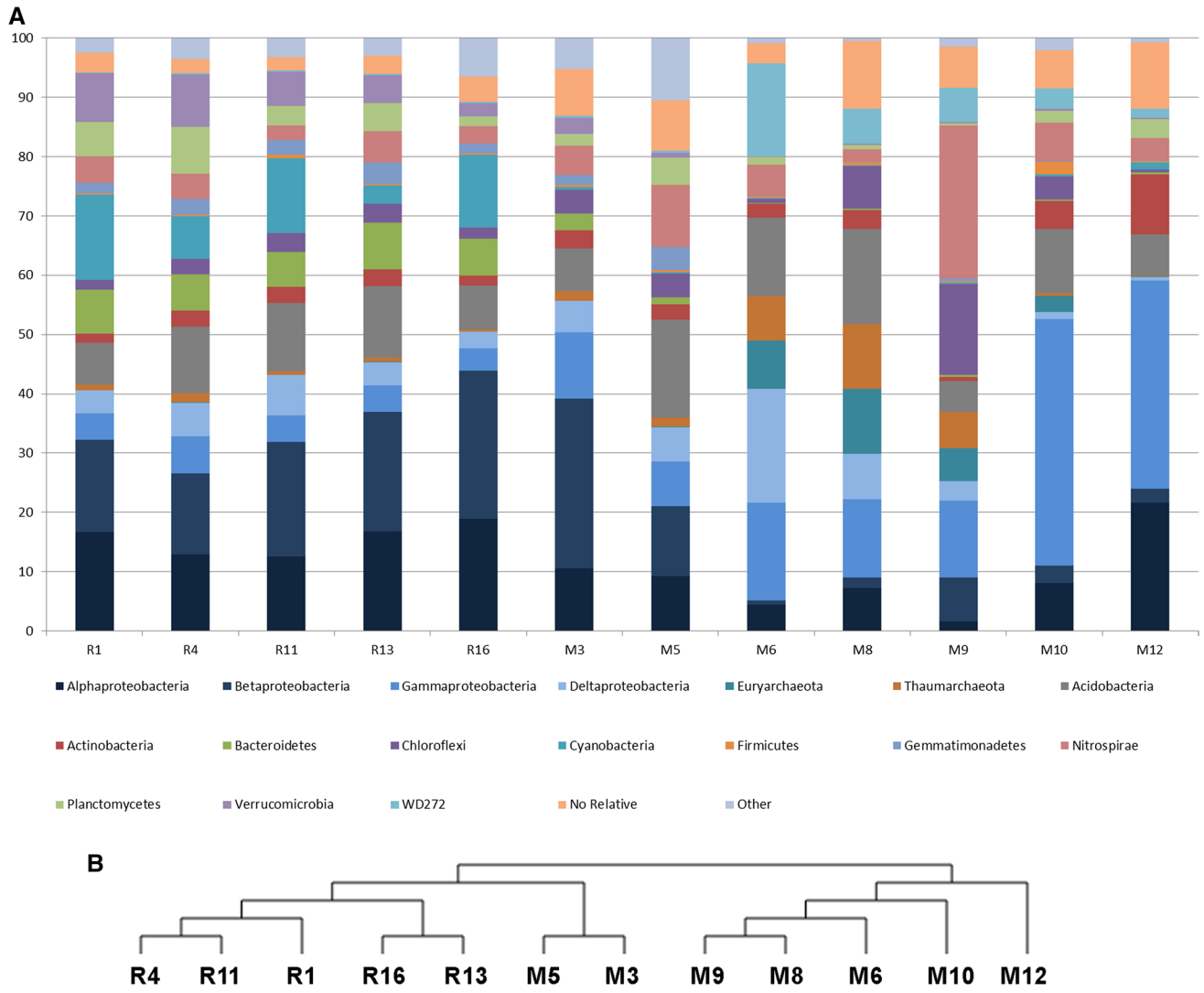

Fig. 3 Prokaryotic community structure performed with 16S rRNA gene metagenomics sequences at phylum and class levels (**a**) and dendrogram according to microbial similarity among samples obtained through MG-RAST server (**b**)

gallery (M3 and M5), characterized by pH values around 4.65 and 7.98. *Alphaproteobacteria* (1.6–20.3%) was abundant in samples that were taken in presence of sunlight (stream samples). *Nitrospirae* (2.1–25.8%), *Chloroflexi* (0.4–15.2%), *Deltaproteobacteria* (0.6–19.2%), *Thaumarchaeota* (0.1–10.9%), *Euryarchaeota* (0.0–11.0%) and Uncultured *WD272* (0.1–15.7%) were abundant in samples M6, M8 and M9 (lateral galleries) which presented high concentrations of soluble Ni, Mn, Fe, Hg, Cu and As. Phyla and classes relative abundances are presented in Online Resource 4.

At the lowest levels, samples M10 and M12 showed the genus *Metallibacterium* from *Gammaproteobacteria* as the most abundant one (> 20%), followed by *Acidibacter* (5–10%). The *Alphaproteobacteria Acidiphilium* was abundant (16%) only in M12 sample. Other taxa well-represented in both M10 and M12 samples included *Actinobacteria* from the *Acidimicrobiales* order and the *Leptospirillum* genus from the *Nitrospirae* phylum. *Leptospirillum* genus was dominant in the M9 sample (25%), followed by *Chloroflexi* from the *Ktedonobacterales* order (10%). Other abundant taxa in M9 were also shared with M6 and M8, including members of phylum *WD272* (6–15%), and *Archaea* from *Thermoplasmatales* order (5–11%) and *Thaumarchaeota* phylum (2–8%). Finally, M6 and M8 samples shared the *GR-WP33-30* order from *Deltaproteobacteria* (18 and 7%, respectively), *Acidobacteria* (6 and 14%), and *Xanthomonadales* (13 and 5%). On the other hand, only a handful of taxa had abundances above 5% in the stream samples, including the *Alphaproteobacteria Novosphingobium* (8%), the *Cyanobacteria Pseudanabaena* (6%) and *Betaproteobacteria* from the family *Comamonadaceae* (6%), all in sample

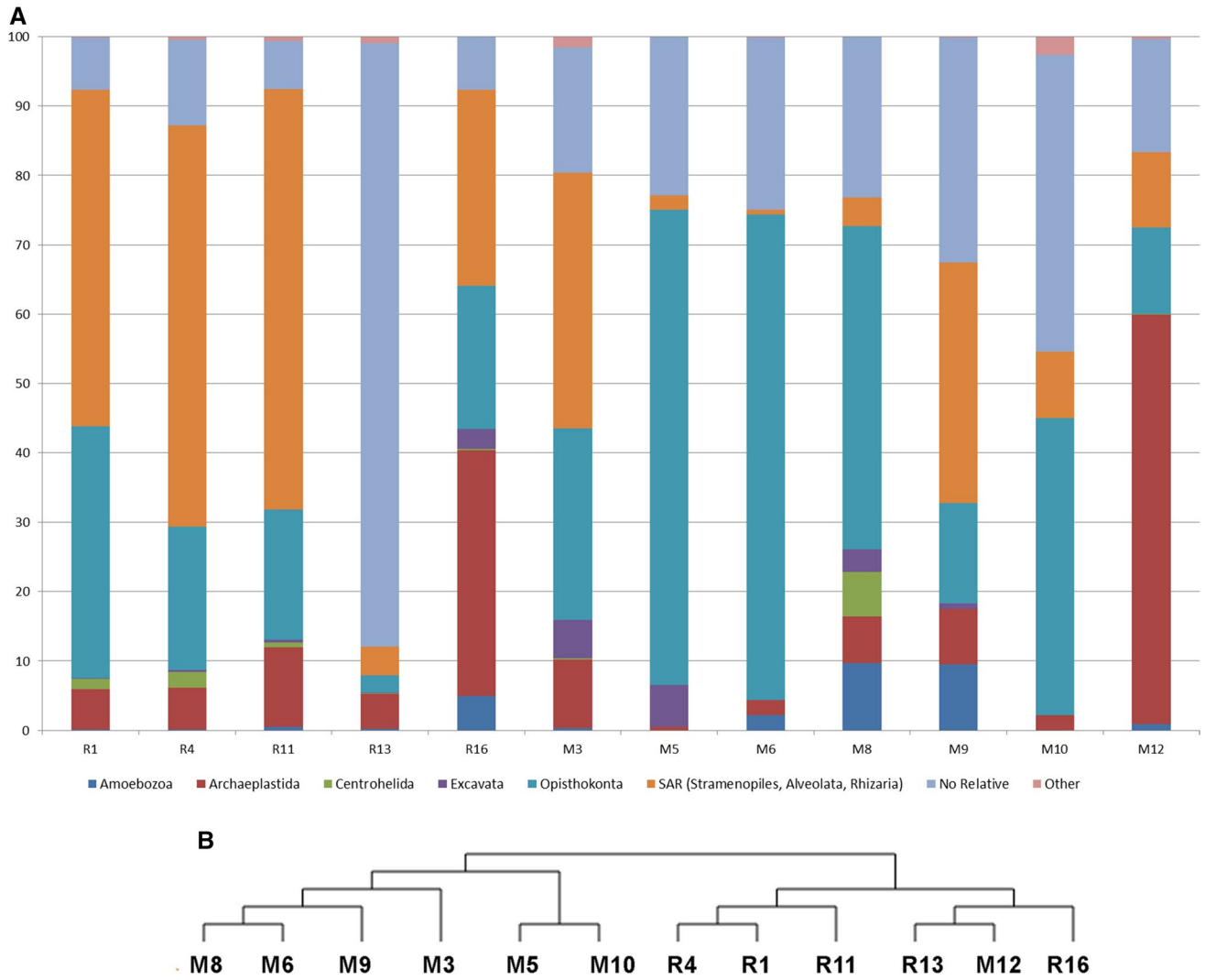

Fig. 4 Eukaryotic community structure performed with 18S rRNA gene metagenomics sequences classified at 93% identity to database sequences (**a**) and dendrogram according to microbial similarity among samples obtained through MG-RAST server (**b**)

R16. It was difficult to find representative members from the different samples. A few more taxa with abundances over 2% in the stream samples, on average, included *Nitrospirae,* members of the families *Nitrosomonadaceae* and *Gemmatimonadaceae*, *Verrucomicrobia*, and *Acidobacteria* (Online Resource 5).

These results suggested a strong correlation between the pH values and the prokaryotic community structure. This was reflected in the abundances among samples, where organisms known to thrive in acidic environments dominated the mine samples (lateral and south galleries) with *Metallibacterium, Acidiphilium*, *Acidibacter* and *Leptospirillum* genera. In these samples, sulfate concentrations were maximal and soluble heavy metals were also important.

The CCA applied on 18S rRNA gene sequences is shown in Fig. 6. Sample M12 was characterized by the presence of *Charophyta* phylum algae (taxa 3 and 16), with a low pH value when in the sunlight. Sample M3 displayed mainly protozoa genus such as *Bromeliophyra* (66), *Heteromita* (68) and *Metopion* (78), neutral pH and lower heavy metal concentrations than the other samples. Green algae from classes *Chlorophyceae* (7) and *Trebouxiophyceae* (19) were associated with samples R13 and R16, characterized by light presence and a pH between 4.65 and 4.86. Different diatoms genera such as *Navicula* (2), *Achnanthidium* (12), *Nitzschia* (44), *Pinnularia* (50), *Cymbella* (72) and *Sellaphora* (83) were found in samples taken up-stream from the south gallery (R1, R4 and R11). These samples presented different green algae genus such as *Staurodesmus* (75), *Staurastrum* (45) and *Hazenia* (25). Samples M5, M6, M8, M9 and M10 were characterized principally by fungi members such as *Malassezia* (8), *Hypocreales* (9), *Sporothrix* (14), *Cibiessia* (34) *Wickeramomyces* (58), *Aspergillus* (82) *and Synchytrium* (76). These samples also showed protists members such as *Centrohelida* (33), *Cercozoa* (73)

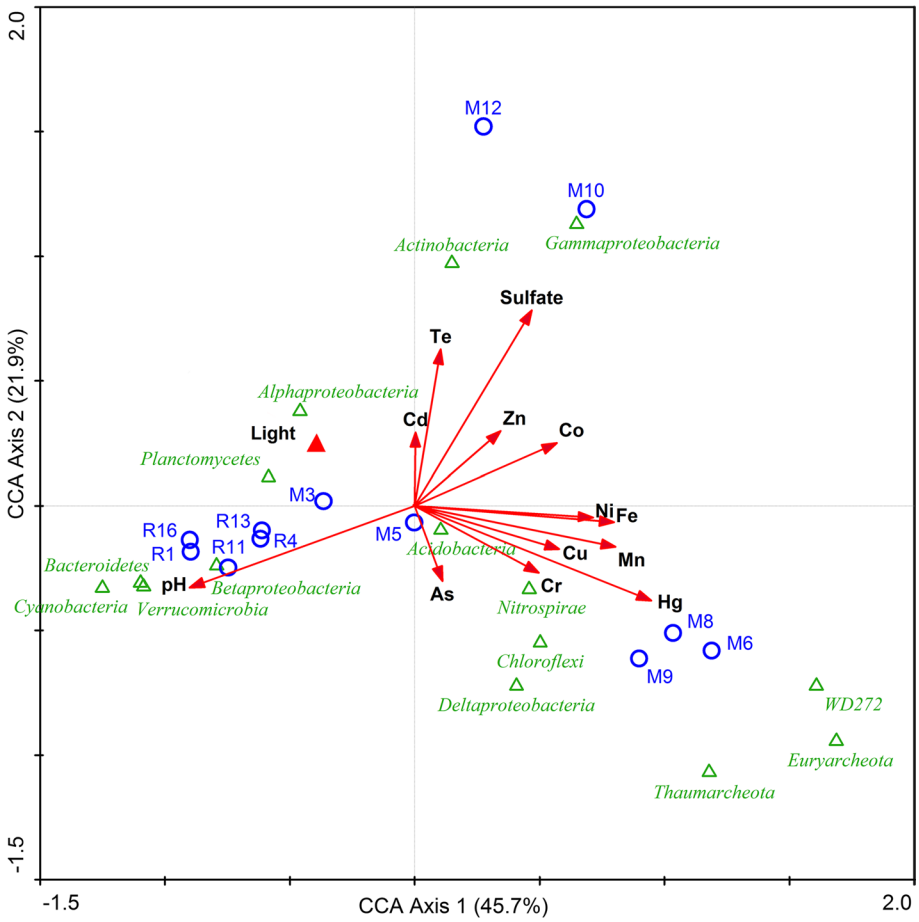

Fig. 5 Canonical Correspondence Analysis (CCA) performed on physicochemical data and 16S rRNA gene metagenomics sequences at phylum and class levels

and *Naegleria* (39). Taxonomic groups not described here correspond to higher eukaryotes organisms (Online Resource 6). From these results obtained with 18S rRNA gene sequences, it can be observed that although there are significant differences in physicochemical parameters among samples, it is clear that the greatest impact on eukaryotic community structure is given by the presence or absence of sunlight. All samples taken in the light (stream samples and M12) were grouped together and they presented algae (green algae and diatoms) as the most abundant microorganisms. Nevertheless, those samples taken in the absence of sunlight (galleries samples) were grouped together and showed fungi and protists as the most abundant microorganisms. It is also interesting to observe that after receiving the AMD, the down-stream samples presented a decrease in the diatoms abundance and green algae predominated.

Discussion

It is known that soils and sediments represent a complex and dynamic matrix of biotic and abiotic components that may influence the bioavailability of sediment-associated chemicals. There are numerous sediment quality guidelines (SQGs) used around the world that establish the limit of chemical substance concentrations that sediments should have to be safety to biological organisms. Most of them have been developed in North America since 1980 (Burton 2002) and currently, they are not available in Latin America. Additionally, these guidelines use total heavy metal concentrations to establish safety limits, and not concentrations which are soluble. Considering this fact, guidelines that take into account soluble heavy metal concentrations still need to be developed (CCME 2001).

Among all parameters that might affect transport of heavy metals in soil systems, the pH is usually considered to be of prime importance (Kuang et al. 2013). For example, when pH decreases, the solubility of heavy metals increases. For this reason, when a microbial community structure study is intended, it is essential to take into account parameters such as pH and soluble heavy metals, among other important factors such as ionic strength and compounds present, since these metals are the ones that have a direct contact with the microbial community, exerting a selection pressure and affecting the community structure and abundance of each of the microorganisms.

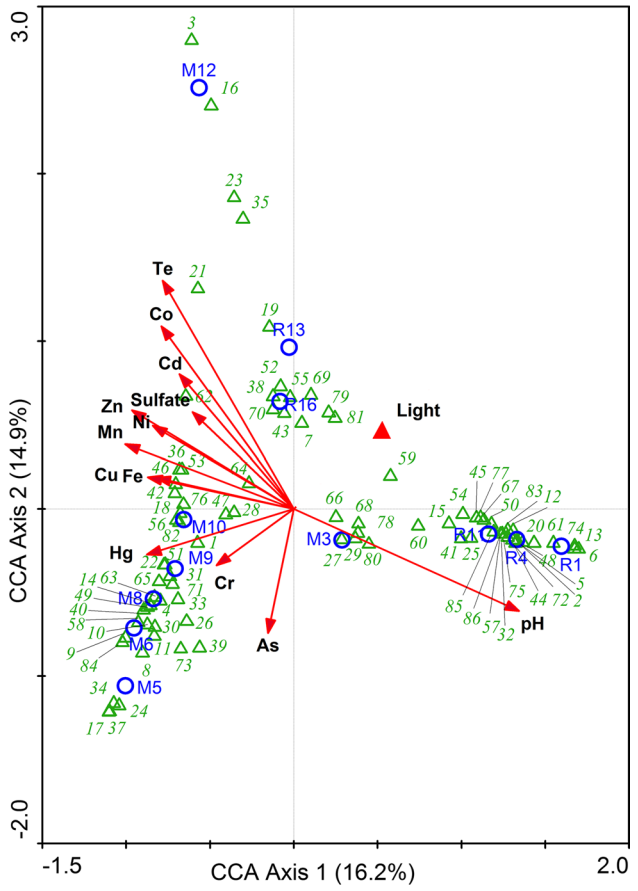

Fig. 6 Canonical Correspondence Analysis (CCA) performed on physicochemical data and 18S rRNA gene metagenomics sequences at the lowest taxonomic levels obtained

There has been much research devoted to the analysis of microbial community structure in contaminated zones, affected by the presence of heavy metals or by AMDs released into natural environments. Most of these studies have focused only on the bacterial community structure and only a few have shown eukaryotic community structure analyses. Due to the rapid microbial response to environmental condition changes, microbial community structure studies could be used to monitor the outcome of bioremediation/bioreclamation efforts applied on affected environments (Hallberg 2010).

Prokaryotic community structure analysis

In the present work, prokaryotic phyla detected in the environment affected by an AMD released from the abandoned gold mine in La Carolina and their relative abundance were: *Proteobacteria* (42.6%) > *Acidobacteria* (10.3%) > *Nitrospirae* (6.5%) > *Cyanobacteria* (4.3%) > *Chloroflexi* (3.9%) > *Bacteroidetes* (3.2%) > *Actinobacteria* (3.1%) > *Planctomycetes* (3.0%) > *Verrucomicrobia* (2.9%) > *WD 272* (2.8%) > *Thaumarchaeota* (2.7%) > *Euryarchaeota* (2.3%).

Some pieces of work focused on the prokaryotic community structure analysis in extreme environments related to sites contaminated by mining activities have been carried out employing different techniques. For example, Hao et al. (2010) studied the composition of prokaryotic communities in AMD associated with pyrite mine tailings in China through library constructions, and Auld et al. (2013) characterized bacterial community from an AMD tailing pond using both culturing and pyrosequencing methods, while Kuppusamya et al. (2016) focused on the study of bacterial community structure in soils contaminated with heavy metals and polycyclic aromatic hydrocarbons, also using pyrosequencing technology. Currently, MiSeq (Illumina Inc., San Diego, CA, USA) is one of the most used platforms for massive parallel sequencing in the assessment of soil microbial community structure through independent-culture techniques (Rincon-Florez et al. 2013). Kuang et al. (2013) analyzed microbial community structure in AMDs and environmental conditions that affected this community structure. In the same line of research, Méndez-García et al. (2015) analyzed prokaryotic and eukaryotic community structure in AMD environments, while Chaput et al. (2015) studied microbial population from passive Mn(II) removal beds that oxidize soluble Mn(II) to insoluble Mn(III/IV) in abandoned coal mines that contain high manganese levels. In all these studies, *Proteobacteria* phylum was the main prokaryotic group, with relative abundances between 40 and 70%.

In agreement with Chaput et al. (2015), who detected *Proteobacteria* from alpha and beta classes at 46.9%, our findings indicate that *Proteobacteria* phylum was the most abundant one at 42.6%. In the above cited works phyla *Acidobacteria*, *Nitrospirae*, *Cyanobacteria*, *Chloroflexi*, *Bacteroidetes*, *Actinobacteria* and *Verrumicrobia* were also found in different proportions. Phyla *Planctomycetes* (García-Moyano et al. 2015), *Thaumarcheota* and *Euryarcheota* (Gupta et al. 2017) also appear related to AMD affected environments.

Kuang et al. (2013) established that pH was the major factor for the patterns of community structure, showing that high values of diversity index were observed in high pH conditions. They found that *Betaproteobacteria* showed low relative abundance in extremely acid environments and predominant abundance under moderate pH conditions. *Alphaproteobacteria, Euryarchaeota, Gammaproteobacteria* and *Nitrospirae* increase their relative abundance in acidic environments. The results of our work are in agreement with those obtained by these authors. Taking into consideration the results obtained from PCA and CCA with the parameters determined in this work, we also propose pH as the major factor affecting prokaryotic community structure. Low pH favored the presence of *Actinobacteria* and

Gammaproteobacteria, while *Betaproteobacteria* presented the highest abundance in samples with pH values close to neutral. *Nitrospirae, Euryarchaeota, Chloroflexi, Deltaproteobacteria, Thaumarchaeota* and Uncultured *WD272* seem to be associated with samples of lateral galleries, which also presented low pH values.

Jackson et al. (2015) showed that the presence of soluble heavy metals and AMD from mine tailings affected community structure of water and sediment samples taken from a polluted lake. Mine waste favored the growth of *Holophagal Acidobacteria*, green sulfur bacteria and *Alphaproteobacteria,* but inhibited a large number of other types of microorganisms resulting in a biodiversity decrease in affected areas. *Holophagal Acidobacteria* increased with low pH and high sulfate concentration. In another study by Kuppusamya et al. (2016), correlation between presence of heavy metals and bacterial phyla was established. Cu, Zn, As and Pb were associated with *Chloroflexi* phylum. Associations between Al and *Proteobacteria,* and among Cr, Ni and *Firmicutes* were also observed. On the other hand, metals like Zn, As, Cd and Pb had a very important effect on the abundance of *Gemmatimonadetes*. In this work, *Nitrospirae, Euryarchaeota, Chloroflexi, Deltaproteobacteria, Thaumarchaeota* and Uncultured *WD272* were associated with Ni, Mn, Fe, Hg, Cu and As.

The most abundant genera found in mine samples in this work were *Metallibacterium, Acidiphilium*, *Acidibacter* and *Leptospirillum.* Members of the *Acidibacter* genus are known to be acidophilic ferric iron-reducing microorganisms and they have been found in metal mines (Falagán and Johnson 2014). *Acidiphilium* and *Leptospirillum* members have been found as microorganisms of a mining consortium isolated directly from copper mines in Chile (Latorre et al. 2016). Likewise, *Metallibacterium* genus appear associated to AMD affected environments as acidophilic Fe-metabolizing bacteria (Sun et al. 2016). These genera have a very important role in the metabolism of the ferric ion, the predominant oxidant agent found in AMD affected environments.

Eukaryotic community structure analysis

As mentioned above, only few studies have focused on eukaryotic community structure analysis of environments affected by anthropogenic activities such as mining. The present work shows that a large number of microbial eukaryotic members are related to fungi, protists, green algae and diatoms. These results are similar to those obtained by other research groups that have described eukaryotic members of AMD affected zones.

Hao et al. (2010) performed an eukaryotic analysis in an AMD affected zone in China and showed that 83% of sequences belonged to phylum *Alveolata,* 11% belonged to family *Nucleariidae,* while about 6% of sequences shared identity with *Penicillium* genus (*Ascomycota* phylum). The study carried out by Chaput et al. (2015) in abandoned coal mines found that fungal sequences in these environments belonged to phyla *Basidiomycota* (47.4%), *Ascomycota* (38.8%), and *Zygomycota, Chytridiomycota* and *Glomeromycota* appeared in abundances below 5%. Half of algae sequences were classified as phylum *Chlorophyta* (green algae), while the next most abundant phylum was *Bacillariophyta* (diatoms). Méndez-García et al. (2015) has carried out the most complete analysis regarding eukaryotic community structure of AMD environments. These authors conclude that microorganisms inhabiting these environments belong mainly to *Archaeplastida*, SAR (*Stramenophiles, Alveolates, Rhizaria*), *Excavata* (protists) and *Opisthokonta* taxa. *Archaeplastida* members present in AMD environments are phototrophic red (*Rhodophyceae*) and green algae (*Chlorophyta*), which depend on sunlight and are found in open-air systems. SAR members include diatoms, ciliates and cercomonads. According to these authors, *Heterolobosea*, *Naegleria* and *Vahlkampfia* were found as *Excavata* members, while *Rotifera* and *Fungi* (*Ascomycota* and *Basidiomycota)* could also be identified as *Opisthokonta* members in these conditions. In an AMD affected site in Northern Ontario, Canada, Auld et al. (2017) have recently found that microorganisms of this environment belonged to algae (*Chrysophyceae*) and fungi members (*Microbotrymycetes* and LKM11).

In this work, we also observed a reduction in the diatom abundance and predominance of green algae members in the down-stream samples after receiving the AMD. The adverse conditions in the AMD affected environments are known to limit the diatom diversity. Diatoms are strongly influenced by acidic environments with pH around 3.0, as shown by Brake et al. (2004) and Schowe et al. (2013). Ochreous precipitates are present in La Carolina stream, after receiving the acid drainage from the south gallery. The Fe(III)-minerals in AMD affected environments are often composed by schwertmannite, ferrihydrite and goetithe, and their formation is favored by the acidic environment conditions (Carlson et al. 2002). The presence of these minerals can affect the microbial communities (Mauck and Roberts 2007). In this sense, Mori et al. (2015) observed a strong relationship between green algae and Fe(III)-precipitates, such as schwertmannite and ferrihydrite. This could also be taking place in our system, as green algae predominate in down-stream samples, which correlates to the presence of Fe(III)- precipitates.

To the best of our knowledge, there are no reports regarding the correlation between eukaryotic groups and environmental conditions of AMD affected environments in sediments, but there are studies performed in water (Amaral-Zettler et al. 2011; Auld et al. 2017). In this work, we established that the presence of light was the major factor that

produced the differences in eukaryotic community structure among samples, affecting mainly algae members (green algae and diatoms). Mesa et al. (2017) also found that sunlight affected the diversity of eukaryotes, and observed the highest diversity in water samples taken under the influence of sunlight in the AMD from Los Ruedos mine, Spain. Additionally, we observed that eukaryotic groups were associated with physicochemical characteristics of the environment.

Conclusions

The present work is an interesting report that establishes specific relationships between physicochemical parameters of AMD affected environments and both eukaryotic and prokaryotic microbial community structure from sediment analysis. This has been achieved using a current massive parallel sequencing platform, i.e., MiSeq, making this study a comprehensive analysis. With our increased understanding of the microbial population of AMD affected environments, a greater understanding of the biogeochemistry is possible, with the potential application of bioremediation processes in a more specific manner, isolating endogenous microorganisms from specific sites.

Acknowledgements The authors would like to thank the English Scientific Writing Advice Group (GAECI) of the National University of San Luis for the revision of this article. Bonilla JO thanks CONICET for the awarded doctoral fellowship.

Funding This work was supported by financial assistance of the National Agency for Scientific and Technological Promotion, Argentina [PICT 2013 No. 3170 to Dr. Villegas].

Compliance with ethical standards

Conflicts of interest The authors declare no conflicts of interest.

References

Amaral-Zettler LA, Zettler ER, Theroux SM, Palacios C, Aguilera A, Amils R (2011) Microbial community structure across the tree of life in the extreme Río Tinto. ISME J 5:42–50

Auld RR, Myre M, Mykytczuk NC, Leduc LG, Merritt TJ (2013) Characterization of the microbial acid mine drainage microbial community using culturing and direct sequencing techniques. J Microbiol Methods 93:108–115

Auld RR, Mykytczuk NC, Leduc LG, Merritt TJ (2017) Seasonal variation in an acid mine drainage microbial community. Can J Microbiol 63(2):137–152

Bond PL, Smriga SP, Banfield JF (2000) Phylogeny of microorganisms populating a thick, subaerial, predominantly lithotrophic biofilm at an extreme acid mine drainage site. Appl Environ Microbiol 66(9):3842–3849

Brake SS, Hasiotis ST, Dannelly HK (2004) Diatoms in acid mine drainage and their role in the formation of iron-rich stromatolites. Geomicrobiol J 21(5):331–340

Burton G Jr (2002) Sediment quality criteria in use around the world. Limnology 3:65–75

Canadian Council of Ministers of the Environment (2001) Canadian sediment quality guidelines for the protection of aquatic life. http://www.ccme.ca/en/resources/canadian_environmental_quality_guidelines/. Accessed 4 Nov 2017

Carlson L, Bigham JM, Schwertmann U, Kyek A, Wagner F (2002) Scavenging of As from acid mine drainage by schwertmannite and ferrihydrite: a comparison with synthetic analogues. Environ Sci Technol 36:1712–1719

Chaput DL, Hansel CM, Burgos WD, Santelli CM (2015) Profiling microbial communities in manganese remediation systems treating coal mine drainage. Appl Environ Microbiol 81:2189–2198

Edwards KJ, Gihring TM, Banfield JF (1999) Seasonal variations in microbial populations and environmental conditions in an extreme acid mine drainage environment. Appl Environ Microbiol 65(8):3627–3632

EPA United States Environmental Protection Agency (2017) Abandoned mine lands: basic information. https://www.epa.gov/superfund/abandoned-mine-lands-basic-information-0. Accessed 4 Nov 2017

Fadiran AO, Dlamini CL, Thwala JM (2014) Environmental assessment of acid mine drainage pollution on surface water bodies around Ngwenya Mine, Swaziland. J Environ Prot 5:164–173

Falagán C, Johnson DB (2014) *Acidibacter ferrireducens* gen. nov., sp. nov.: an acidophilic ferric iron-reducing gammaproteobacterium. Extremophiles 18(6):1067–1073

García-Moyano A, Erling Austnes A, Lanzén A, González-Toril E, Aguilera Á, Øvreås L (2015) Novel and unexpected microbial diversity in acid mine drainage in Svalbard (78° N), revealed by culture-independent approaches. Microorganisms 3:667–694

Gupta A, Dutta A, Sarkar J, Paul D, Panigrahi MK, Sar P (2017) Metagenomic exploration of microbial community in mine tailings of Malanjkhand copper project, India. Genom Data 12:11–13

Hallberg KB (2010) New perspectives in acid mine drainage microbiology. Hydrometallurgy 104:448–453

Hao C, Wang L, Gao Y, Zhang L, Dong H (2010) Microbial diversity in acid mine drainage of Xiang Mountain sulfide mine, Anhui Province, China. Extremophiles 14:465–474

Hernandez AJ, Pastor J (2008) Relationship between plant biodiversity and heavy metal bioavailability in grasslands overlying an abandoned mine. Environ Geochem Health 30:127–133

Jackson TA, Vlaar S, Nguyen N, Leppard GG, Finan TM (2015) Effects of bioavailable heavy metal species, arsenic, and acid drainage from mine tailings on a microbial community sampled along a pollution gradient in a freshwater ecosystem. Geomicrobiol J 32:724–750

Jennings SR, Neuman DR, Blicker PS (2008) Acid mine drainage and effects on fish health and ecology: a review. Reclamation Research Group Publication, Bozeman

Johnson DB, Hallberg KB (2003) The microbiology of acidic mine waters. Res Microbiol 154:466–473

Kirschbaum A, Murray J, Arnosio M, Tonda R, Cacciabue L (2012) Pasivos ambientales mineros en el noroeste de Argentina: aspectos mineralógicos, geoquímicos y consecuencias ambientales. Revista Mexicana de Ciencias Geológicas 29(1):248–264

Kuang JL, Huang LN, Chen LX, Hua ZS, Li SL, Hu M et al (2013) Contemporary environmental variation determines microbial diversity patterns in acid mine drainage. ISME J 7:1038–1050

Kuppusamya S, Thavamanic P, Megharaj M, Venkateswarlu K, Lee YB, Naidub R (2016) Pyrosequencing analysis of bacterial diversity in soils contaminated long-term with PAHs and heavy metals: implications to bioremediation. J Hazard Mater 317:169–179

Latorre M, Cortés MP, Travisany D, Di Genova A, Budinich M, Reyes-Jara A, Hödar C et al (2016) The bioleaching potential of a bacterial consortium. Bioresour Technol 218:659–666

Mauck BS, Roberts JA (2007) Mineralogic control on abundance and diversity of surface-adherent microbial communities. Geomicrobiol J 24:167–177

Méndez-García C, Peláez AI, Mesa V, Sánchez J, Golyshina OV, Ferrer M (2015) Microbial diversity and metabolic networks in acid mine drainage habitats. Front Microbiol 6:475

Mesa V, Gallego JLR, González-Gil R, Lauga B, Sánchez J, Méndez-García C, Peláez AI (2017) Bacterial, archaeal, and eukaryotic diversity across distinct microhabitats in an acid mine drainage. Front Microbiol 8:1756

Meyer F, Paarmann D, D´Souza M, Olson R, Glass EM, Kubal M et al (2008) The metagenomics RAST server—a public resource for the automatic phylogenetic and functional analysis of metagenomes. BMC Bioinform 9:386

Mori JF, Neu TR, Lu S, Händel M, Totsche U, Küsel K (2015) Iron encrustations on filamentous algae colonized by Gallionella-related bacteria in a metal-polluted freshwater stream. Biogeosciences 12:5277–5289

Oblasser A, Chaparro Ávila E (2008) Estudio comparativo de la gestión de los pasivos ambientales mineros en Bolivia, Chile, Perú y Estados Unidos. CEPAL—Serie Recursos Naturales e Infraestructura N° 131. Santiago de Chile, 2008. ISBN: 978-92-1-323175-3

Quast C, Pruesse E, Yilmaz P, Gerken J, Schweer T, Yarza P et al (2013) The SILVA ribosomal RNA gene database project: improved data processing and web-based tools. Nucleic Acids Res 41:D590–D596

Rincon-Florez VA, Carvalhais C, Schenk PM (2013) Culture-independent molecular tools for soil and rhizosphere microbiology. Diversity 5:581–612

Ruggieri F, Gil RA, Fernandez-Turiel JL, Saavedra J, Gimeno D, Lobo A et al (2012) Multivariate factorial analysis to design a robust batch leaching test to assess the volcanic ash geochemical hazard. J Hazard Mater 213–214:279–284

Schowe KA, Harding JS, Broady PA (2013) Diatom community response to an acid mine drainage gradient. Hydrobiologia 705:147–158

Singh M, Ansari AA, Müller G, Singh IB (1997) Heavy metals in freshly deposited sediments of Gomti river (a tributary of the Ganga river): effects of human activities. Environ Geol 29:246–252

Sun W, Xiao E, Krumins V, Dong Y, Xiao T, Ning Z et al (2016) Characterization of the microbial community composition and the distribution of Fe-metabolizing bacteria in a creek contaminated by acid mine drainage. Appl Microbiol Biotechnol 100(19):8523–8535

Tiwari MK, Bajpai S, Dewangan UK, Tamrakar RK (2015) Suitability of leaching test methods for fly ash and slag: a review. J Radiat Res Appl Sci 8:523–537

Tripole ES, Corigliano MC (2005) Acid stress evaluation using multimetric indices in the Carolina stream (San Luis –Argentina). Acta Limnol Bras 17(1):101–114

Tripole S, Gonzalez P, Vallania A, Garbagnati M, Mallea M (2006) Evaluation of the impact of acid mine drainage on the chemistry and the macrobenthos in the Carolina stream (San luis—Argentina). Environ Monit Assess 114:377–389